

An edited version of this paper was published by [AGU](#).

---

## Effect of bandwidth on seismic imaging of rotating stratified turbulence surrounding an anticyclonic eddy from field data and numerical simulations

C. Ménesguen<sup>1,\*</sup>, B. L. Hua<sup>1</sup>, C. Papenberg<sup>2</sup>, D. Klaeschen<sup>2</sup>, L. Géli<sup>3</sup>, R. Hobbs<sup>4</sup>

<sup>1</sup> Laboratoire de Physique des Océans, IFREMER, Plouzané, France

<sup>2</sup> IFM-GEOMAR, Kiel, Germany

<sup>3</sup> Laboratoire de Géodynamique et de Géophysique, IFREMER, Plouzané, France

<sup>4</sup> Department of Earth Sciences, University of Durham, Durham, UK

\*: Corresponding author : C. Ménesguen, email address : [cmenesg@ifremer.fr](mailto:cmenesg@ifremer.fr)

---

### Abstract:

The fine resolution of long geoseismic sections should permit the characterization of oceanic turbulence properties over several decades of horizontal scales. The range of horizontal scales actually probed by three different acoustic sources is found to be directly linked to their frequency content. The horizontal inertial range with a spectral slope of  $k^{-5/3}$  extend up to 3 km wavelength for the most intense acoustic reflectors which surround strong anticyclonic eddies. The in situ data analysis is confirmed by high resolution numerical simulations of oceanic anticyclonic vortices, in a rotating temperature-stratified fluid (no salt), which show the spontaneous emergence of a concentration of acoustic reflectors above and below the eddy. These show an anisotropy and a spectral slope consistent with the framework of stratified turbulence, which differs from that of Garrett and Munk for internal waves. The implications are that a direct energy cascade to smaller spatial scales is occurring at the boundaries of energetic oceanic vortices and may provide a mechanism to drive mixing in the ocean interior.

## 1. Introduction

20 An interesting outcome of the GO (Geophysical Oceanography) experiment [*Hobbs*,  
21 2007] is its successful survey of energetic, long-lived anticyclonic lens-shaped vortices in  
22 the Gulf of Cadiz, known as Meddies. They are particularly abundant in the Mediter-  
23 ranean water outflow in the 700-1500 m depth range [*Armi et al.*, 1989]. Such vortices are  
24 responsible for a large part of the saltier Mediterranean Water tongue in the North Atlantic  
25 and play an essential role for momentum, heat and tracer transport at those depths. In all  
26 available seismic observations, the boundaries of Meddies are marked by a concentration  
27 of acoustic reflectors, vertically-stacked, with a typical vertical lengthscale of 20-40 m and  
28 typical horizontal scales of several tens of kilometers [see detailed review of possible mech-  
29 anisms in *Biescas et al.*, 2008]. The unprecedented horizontal spatial sampling provided  
30 by seismic oceanography invites probing into the nature of the fundamental processes on  
31 the route to dissipation and mixing that may occur near strongly energetic vortices such  
32 as Meddies. It should permit to characterize the properties of oceanic turbulence over  
33 several decades of spatial scales, especially in the horizontal direction.

34 Evidence of horizontal inertial range spectral behavior of  $k_h^{-5/3}$ , where  $k_h$  is the hori-  
35 zontal wavenumber, from direct ocean observations are available. Among the most recent  
36 ones, *Holbrook and Fer* [2005] report geoseismic remote sensing of the internal wave field  
37 in both the open ocean and near the continental rise and note a propensity for a  $k_h^{-5/3}$   
38 behavior for the spectra of the reflector displacement as the more energetic region of the  
39 continental slope is approached. Likewise, in the remote sensing of the internal wave-field  
40 off the Iberian peninsula by *Krahmann et al.* [2008], there is a better fit, for the more

41 energetic regions, to  $k_h^{-5/3}$  for horizontal wavelengths between 200 m and 1.6 km than to  
42  $k_h^{-2}$  characteristic of the Garrett-Munk internal wave spectrum (their Figure 6). Isopyc-  
43 nal displacement spectra near the Hawaiian ridge have been collected using a horizontally  
44 towed vehicle MARLIN by *Klymak and Moum* [2007] who noted a transition between  
45 turbulent regimes. The turbulence inertial-convective subrange corresponding to a -5/3  
46 power law in horizontal energy spectra extends to surprisingly large scales ( $> 500$  m),  
47 when compared to the Ozmidov length beyond which the -5/3 power law associated with  
48 3D isotropic Kolmogorov turbulence is expected.

49 Presently, the interpretation of spectral slopes as due to stratified turbulence versus  
50 random internal waves is still under debate. The framework of “stratified turbulence”  
51 describing the dynamics of quasi-horizontal, meandering motions dominated by stable  
52 density stratification offer a complementary/alternative interpretation to internal waves  
53 for such observations of  $k_h^{-5/3}$ , as elaborated by *Riley and Lindborg* [2008]. The most  
54 recent numerical simulations [reviewed in *Brethouwer et al.*, 2007] as well as scaling  
55 arguments [*Billant and Chomaz*, 2001] have clearly established that a strong downscale  
56 transfer of energy exists in the horizontal and, along with this, that the development of a  
57 horizontal spectral inertial range can occur. A salient result is that the spectra of kinetic  
58 and potential energy display a  $k_h^{-5/3}$  power-law behaviour.

59 A generic feature of stratified turbulence being the presence of quasi-horizontal lay-  
60 ers, it is tempting to relate such patterns to the concentrated “layering” revealed by  
61 seismic oceanography immediately above and below Meddies. However, the “stratified  
62 turbulence” paradigm neglects all rotation effects and the reflectors revealed by seismic

63 oceanography have a long horizontal extension, exceeding tens of kilometers, which is into  
64 the range of “balanced” scales of motion. –The balanced motions are described by an  
65 approximated set of equations which truncates the horizontal divergence equation –. This  
66 begs the question of assessing what is the upper limit of the horizontal inertial range spec-  
67 tral behavior in  $k_h^{-5/3}$  in the GO data set? [*Molemaker et al.*, 2009, provide evidence of  
68 an extension of the  $k_h^{-5/3}$  range to larger, balanced scales that are influenced by rotation,  
69 but for flows without quasi-horizontal layers.] Can the layering phenomena be reproduced  
70 in direct numerical simulations? Does its formation involve the slow balanced dynamics  
71 characterized by the total vorticity component perpendicular to isopycnal surfaces (Po-  
72 tential Vorticity or PV)? Or does the fast dynamics of high frequency unbalanced internal  
73 waves come into play [*Riley and Lelong*, 2000]?

## 2. Data

74 The GO-project acquired a combined seismic and physical oceanography dataset which  
75 repeatedly crossed a Meddy. Two of the profiles are used in this paper, GO-LR-13 and GO-  
76 MR-05 [Fig.1 and Fig.1 of *Krahmann et al.*, 2009]. For GO-LR-13, the 6-airgun source  
77 (total volume of 2320 cu in) was towed at a nominal depth of 10 m and the 2.4 km long  
78 hydrophone receiver array was towed at 8 m. For GO-MR-05, we used a novel dual source  
79 array to provide simultaneous seismic images of the Meddy over two bandwidths. The first  
80 3-airgun 1160 cu in source (Flop) was towed at a nominal depth of 10 m and the second  
81 3-airgun 540 cu in source (Flip) was towed at a nominal depth of 5 m, for both sources  
82 the 2.4 km long hydrophone receiver array was towed at 5 m. The frequency of the Flop  
83 source is comparable to the original low-frequency GO-LR-13 source with a bandwidth

84 of 5-60 Hz (insert Fig.1(b) and Fig.1(a)), though the amplitude of the Flop source is less  
85 as it only used three as opposed to six airguns. The Flip source has a bandwidth of  
86 10-100 Hz (insert Fig.1(c)) and its amplitude is less again because the energy is spread  
87 over a wider bandwidth by using a smaller airgun volume and towing less deep which  
88 makes the source acoustically less efficient. The main processing steps for the seismic  
89 data focused on removing the strong energetic direct wave, preserving signal amplitudes  
90 and correcting source and receiver directivity. The processed data were then migrated,  
91 a seismic processing tool for geometric repositioning, using a true amplitude 3D time  
92 migration algorithm. Figure 1 only reproduces the portion of the water column lying in  
93 the 500-1200 m range and shows the presence of stacked reflectors immediately above the  
94 lens core.

### 3. Model

95 Direct numerical simulations at resolution up to  $1000^3$  grid points have been performed  
96 with the Boussinesq, non hydrostatic code of *Aiki et al.* [2006], which has been tailored  
97 to accommodate the massively parallel, vectorial architecture of the Earth Simulator.  
98 The anisotropic grid is 100 m in the horizontal and 3 m in the vertical directions. A  
99 wide range of numerical simulations has been performed to address the free evolution of  
100 anticyclonic eddies whose spatial characteristics are close to those observed during the  
101 GO cruise (lenses with an inner solid body rotation core of 20-25 km radius, maximal  
102 azimuthal velocity ranging from 12 to 25 cm/s, height of 400-600 m), which are initialized  
103 in cyclogeostrophic balance and for Rossby number ranging from 0.2 to 0.6. Background  
104 rotation correspond to a constant  $f$ -plane, whose inertial period is about 20 hours, typical

105 of the Gulf of Cadiz. We stress that, in all our simulations, the density field variations  
106 are assumed to depend on temperature variations alone and to a constant background  
107 stratification of  $N = 3.3 \cdot 10^{-3} \text{ s}^{-1}$ . No salinity effects are taken into account, so that  
108 there is an a priori assumption that prevents double-diffusion and other thermohaline  
109 mechanisms. We test the possibility of an energy cascade due to a spontaneous loss of  
110 balance of the anticyclonic lens which could involve, as in *Plougonven et al.* [2005], an  
111 instability that couples balanced modes and unbalanced waves. <sup>1</sup> In all the simulations  
112 we observe the spontaneous evolution of step-like distributions in the initially vertically  
113 smooth PV distribution (Fig.2) which occurs between two to four weeks of evolution  
114 depending on the strength of the eddy. Such modifications are characterized by slow  
115 dynamics and cannot be attributed to fast internal gravity waves *alone* since they do not  
116 carry PV [*Riley and Lelong*, 2000].

117 The corresponding distribution of acoustic reflectivity, induced by vertical variations of  
118 the acoustic impedance –which is defined as the product of the fluid density and sound-  
119 speed and largely controlled by temperature anomalies–, is plotted in Figure 3(a). One  
120 can observe that the vertical derivative of temperature signal shapes the PV field. The  
121 convolution of acoustic reflectivity by the Flop and Flip source wavelets yields patterns  
122 shown in Figures 3(b) and 3(c) respectively. Both sources image the induced layering  
123 though the higher frequency Flip source reveals finer vertical layers (especially in the eddy  
124 interior). Moreover, the Flip source also shows a slightly shorter horizontal extension to  
125 the reflectors.

#### 4. Analysis Method

126 To probe for the possible existence of the inertial range in the data, our analysis uses  
 127 second order structure function  $S(r)$  (where  $r$  is horizontal lag) rather than classical  
 128 spectral analysis. <sup>2</sup> Since  $S(r)$  is in Fourier duality with the power spectrum, if there is a  
 129 power law in spectrum,  $E(k_h) \propto k_h^{-n}$ , with  $1 < n < 3$ , then  $S(r) \propto r^{n-1}$ . In the present  
 130 case, a  $-5/3$  (or  $-2$ ) power law in spectra will correspond to a  $+2/3$  (or  $+1$ ) power law in  
 131 structure function.

#### 5. Horizontal Inertial Ranges in $k_h^{-5/3}$

132 We have analysed the GO seismic oceanography data in terms of their second order  
 133 structure function (Fig.4). Calculations are binned inside horizontal 12 km long boxes,  
 134 centered on the most intense acoustic reflectors above the Meddy.

135 The three sections from Figure 1 (GO-LR-13, and GO-MR-05-Flop and -Flip) display a  
 136 range of horizontal scales with parts of the structure functions scaling close to a  $2/3$  power  
 137 law which corresponds to a spectral inertial range in  $k_h^{-5/3}$ . There is a constant power  
 138 law over nearly a decade in all three sections, with a  $2/3$  coefficient for all cases when  
 139 taking into account error bars. Furthermore, an assessment of the convolution of a known,  
 140 synthetic dataset by the different sources shows that it induces a decrease of the slope  
 141 in the structure functions of 0.06 for Flip, 0.02 for Flop and 0.01 for LR. The inertial  
 142 range found for Flip corresponds to smaller horizontal scales than Flop by 25%: this  
 143 moderate shift to smaller scales can be attributed to the higher frequency content of Flip.  
 144 Our evidence is based on reflectivity field which is dominated by the vertical gradient  
 145 of temperature whereas the theoretical framework of stratified turbulence predicts a -

146 5/3 power law for potential energy spectrum. Since in simulations both the temperature  
147 anomalies and their vertical gradient display horizontal inertial ranges in  $k_h^{-5/3}$  for roughly  
148 the same range of horizontal scales, it is plausible that observed power laws are consistent  
149 with stratified turbulence. This result needs to be rationalized in further studies.

## 6. Discussion

150 The regions where the  $k_h^{-5/3}$  inertial range is observed coincide with the high concentra-  
151 tions of the most intense acoustic reflectors immediately above and below the anticyclonic  
152 lenses. The nonuniform distribution of the reflectors is a signature of strong spatial inter-  
153 mittency. The horizontal scales which are concerned lie in the range of 300 m to 2.8 km  
154 for the present acoustic sources and are impacted by the bandwidth of seismic sources. As  
155 *Klymak and Moum* [2007], we find a -5/3 power law horizontal inertial range which also  
156 extends to quite large horizontal wavelength. Actually, the detailed energy diagnostics  
157 of the numerical simulations (not shown) reveal that the upper bound of this -5/3 power  
158 law inertial range can be even larger than 3 km and depends on the flow parameters,  
159 in particular the strength of the anticyclonic lens. A down-scale potential and kinetic  
160 energy transfer to small horizontal scales at the depths coinciding with the concentration  
161 of strong acoustic reflectors has been diagnosed. Such results could be interpreted as  
162 the manifestation of an instability route to dissipation for the ocean interior away from  
163 boundaries [see *Molemaker et al.*, 2009]. Finally, instabilities which occur leads to tur-  
164 bulence with a strong signature in the potential vorticity field, thus involving nonlinear  
165 mechanisms other than free internal waves which leave no trace on potential vorticity.



166 We conclude that seismic oceanography is a significant tool to improve our understand-  
167 ing of the transition in geophysical turbulence regimes between the tens of kilometers scale  
168 balanced motions and the intermediate scales that are involved in the route to dissipation  
169 and mixing. However, the present analysis shows that the frequency content of acoustic  
170 sources has a direct influence on the extension of horizontal inertial range that is actually  
171 sampled, e.g. smaller horizontal scales are kept for the Flip source and larger horizontal  
172 scales for the Flop source.

173 **Acknowledgments.** The GO-project was funded by the European Commission (FP6-  
174 NEST-15603). RWH was a NERC Advanced Research Fellow. This work has benefited  
175 from grant 96130 from IDRIS. Access to the Earth Simulator is through IFREMER-  
176 CNRS-ES MOU. We are grateful to E. Lindborg, S. Le Gentil and Dr. H. Aiki.

## Notes

1. See additional material for more information.

177

2. See additional material for further explanations.

## References

178 Aiki, N., H. Takahashi, and T. Yamagata, The Red Sea out flow regulated by the Indian  
179 monsoon, *Continental Shelf Research*, *26*, 1448–1468, 2006.

180 Armi, L., D. Hebert, N. Oakey, J. Price, P. Richardson, T. Rossby, and R. B., Two years  
181 in the life of a mediterranean salt lens, *J. Phys. Oceanogr.*, *19*, 354–370, 1989.

182 Biescas, B., V. Sallares, J. Pelegri, F. Machin, R. Carbonell, G. Buffett, J. Danobeitia,  
183 and C. A., Imaging meddy finestructure using multichannel seismic reflection data,  
184 *Geophysical Research Letters*, *35*(L033971), 2008.

185 Billant, P., and J. Chomaz, Self-similarity of strongly stratified inviscid flows, *Phys. Fluids*  
186 *A*, *13*, 1645–1651, 2001.

187 Brethouwer, G., P. Billant, E. Lindborg, and J. Chomaz, Scaling analysis and simulation  
188 of strongly stratified turbulent flows, *J. Fluid Mech.*, *585*, 342–368, 2007.

189 Hobbs, R., GO (geophysical oceanography): A new tool to understand the  
190 thermal structure and dynamics of oceans, *European Union Newsletter*, *2*,  
191 <http://www.aapg.org/europe/newsletters/2007/06jun/06jun07europe.pdf>, 2007.

192 Holbrook, W., and I. Fer, Ocean internal wave spectra inferred from seismic reflection  
193 transects, *Geophysical Research Letters*, *32*, 2005.

- 194 Klymak, J., and J. Moum, Oceanic isopycnal slope spectra: Part ii - Turbulence, *J. Phys.*  
195 *Oceanogr.*, *301*, 1232–1245, 2007.
- 196 Krahmman, G., P. Brandt, D. Klaeschen, and T. Reston, Mid-depth internal wave energy  
197 off the Iberian peninsula estimated from seismic reflection data, *J. Geophys. Res.*, *113*,  
198 C12,016, 2008.
- 199 Krahmman, G., C. Papenberg, P. Brandt, and M. Vogt, Evaluation of seismic reflector  
200 slopes with a yoyo-ctd, *Geophysical Research Letters*, special issue, in press, 2009.
- 201 Molemaker, M., J. McWilliams, and X. Capet, Balanced and unbalanced routes to dissi-  
202 pation in an equilibrated Eady flow, *J. Fluid Mech.*, in press, 2009.
- 203 Plougonven, R., D. Muraki, and C. Snyder, A baroclinic instability that couples balanced  
204 motions and gravity waves, *J. Atmos. Sci.*, *62*(1545-1559), 2005.
- 205 Riley, J., and M.-P. Lelong, Fluid motions in the presence of strong stable stratification,  
206 *Annu. Rev. Fluid Mech.*, *32*(613-657), 2000.
- 207 Riley, J., and E. Lindborg, Stratified turbulence: A possible interpretation of some geo-  
208 physical turbulence measurements, *J. Atmos. Sci.*, *65*(24162424), 2008.

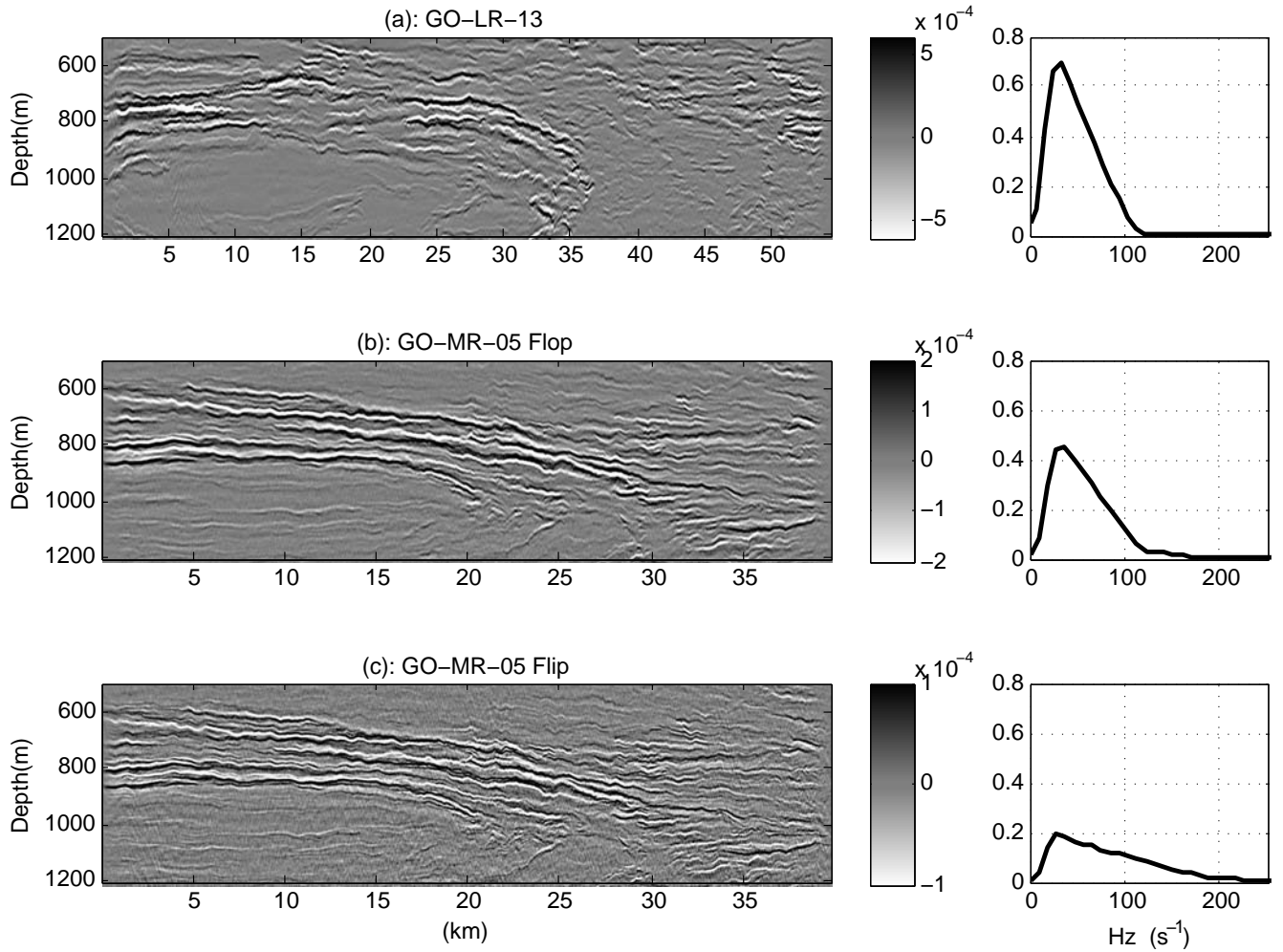


**Figure 1.** Seismic sections of reflexion coefficients (unitless) convolved with: (a) LR-13, (b) Flop (c) Flip, with the source wavelet spectrum (right) indicating the approximate relative amplitude of the different air gun sources.

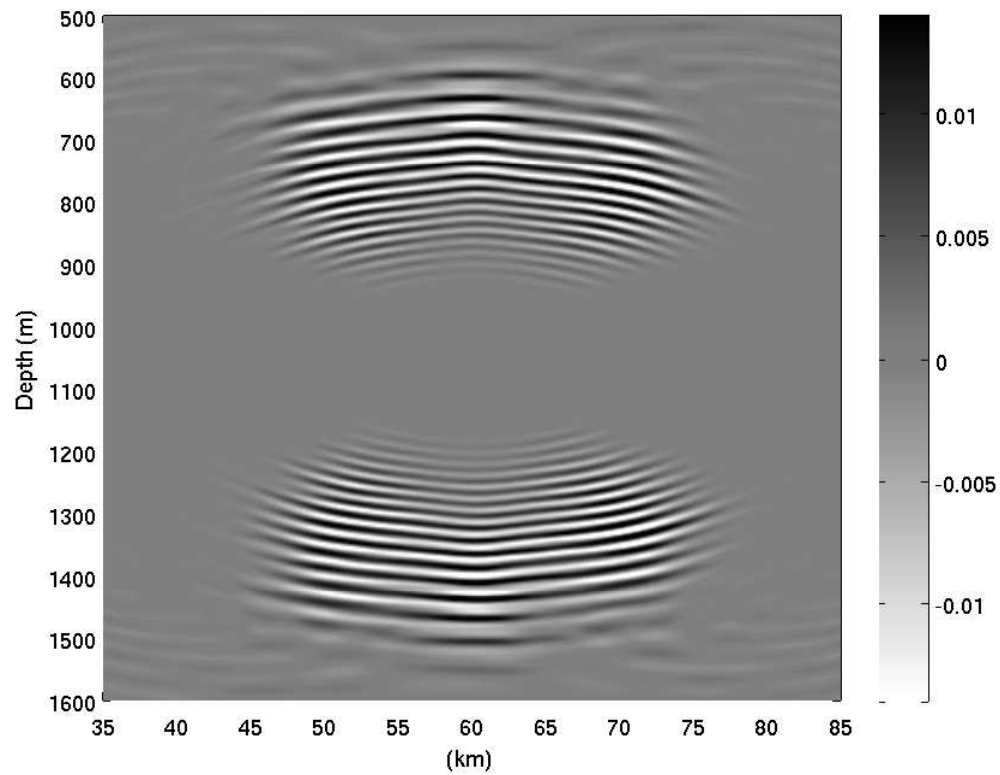


**Figure 2.** Numerical simulations of an anticyclonic eddy with maximal azimuthal velocity of 1 cm/s and a solid body rotation core radius of 20 km: potential vorticity field across the eddy center.

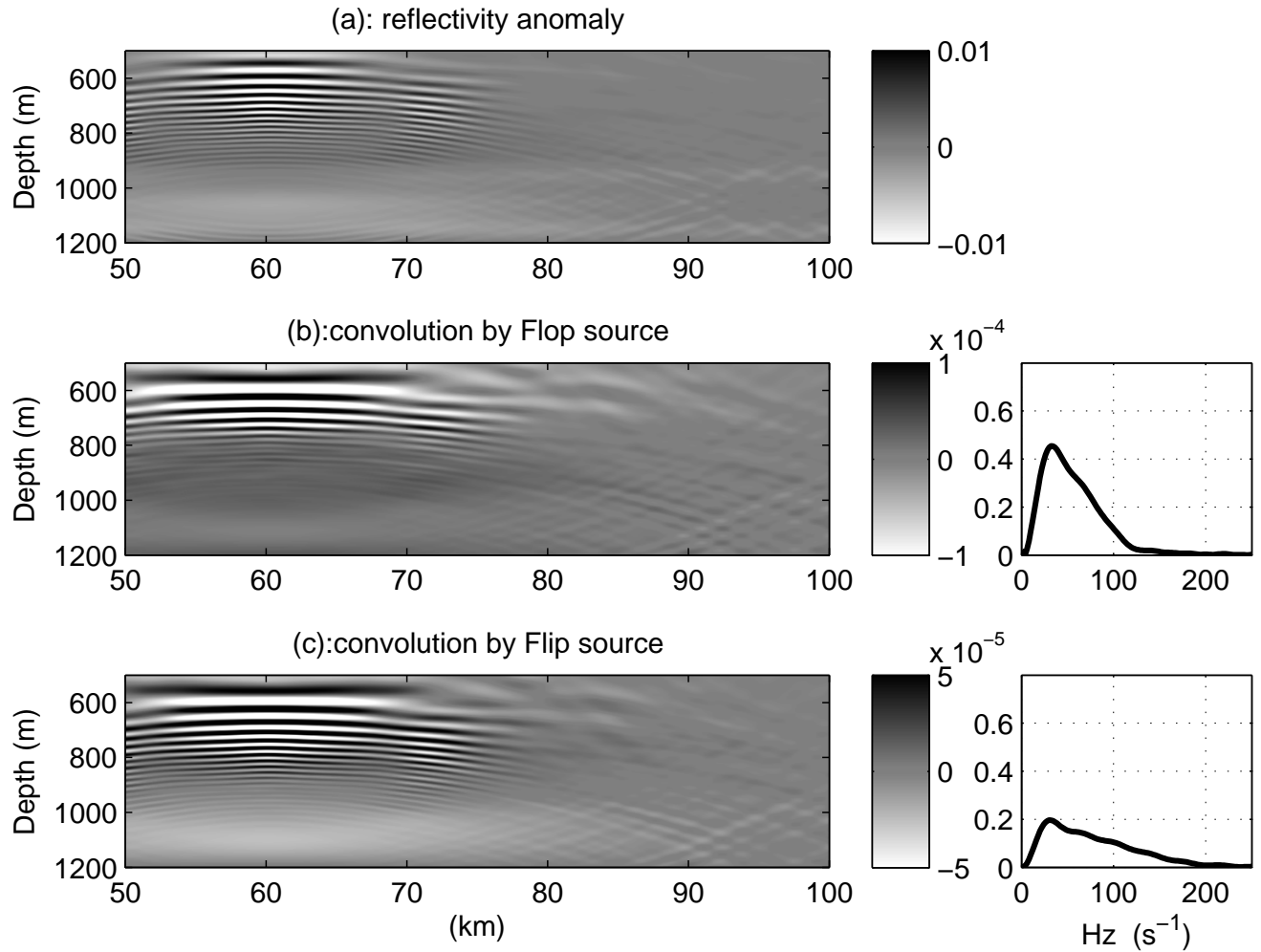


**Figure 3.** Numerical simulations of an anticyclonic eddy with maximal azimuthal velocity of 21 cm/s and a solid body rotation core radius of 20 km: **(a)** Reflectivity anomaly, **(b)** Reflectivity convoluted by Flop wavelet **(c)** Reflectivity convoluted by Flip wavelet, with on the right the spectrum of the corresponding source wavelet.

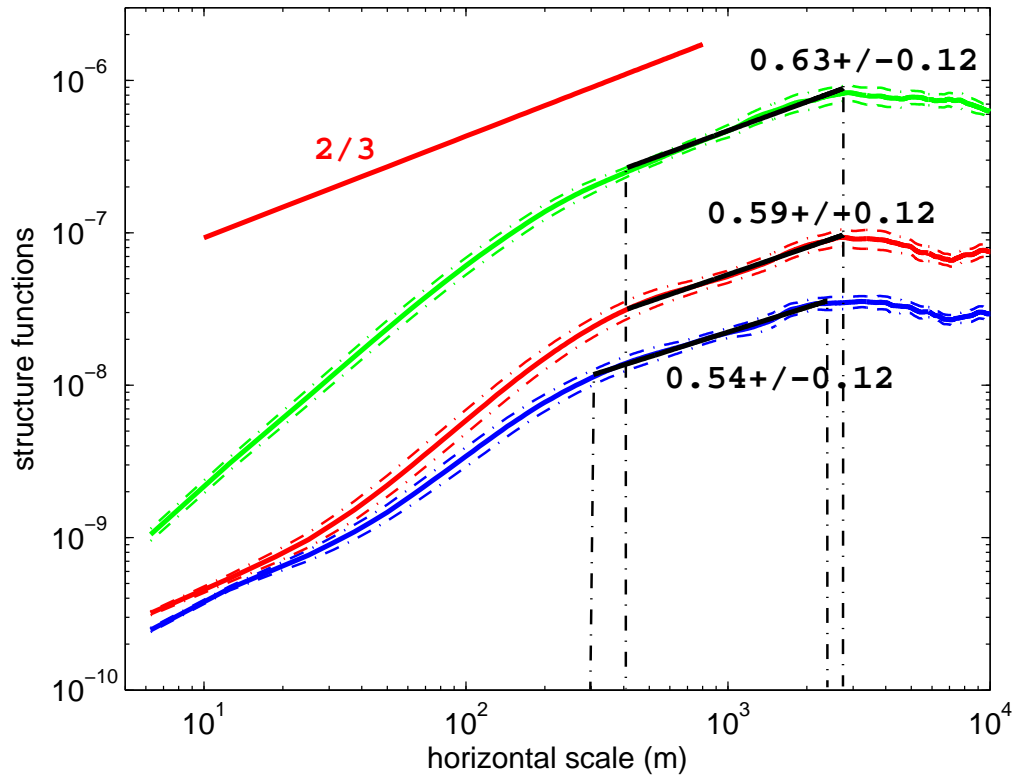


**Figure 4.** Second order structure functions for the different geoseismic sections of Figure 1 (green: LR-13, red: Flop, blue: Flip), with standard deviation in colored dash lines. Black lines are best power law fits whose exponent is to be compared with  $2/3$ . For all three cases, the  $+2/3$  power law lies within the error bars of the structure functions. The difference in magnitude between the three different curves is due to differences in the intensity of the air gun sources.